10.10 AN IMPROVED GUST FRONT DETECTION CAPABILITY FOR THE ASR-9 WSP

Seth Troxel*, Bob Frankel, Beth Echels, Cindy Rolfe
MIT Lincoln Laboratory, Lexington, Massachusetts

1. INTRODUCTION†

The Weather Systems Processor (WSP) is being deployed by FAA at 35 medium and high-density ASR-9 equipped airports across the United States. The Machine Intelligent Gust Front Algorithm (MIGFA) developed at Lincoln Laboratory provides important gust front detection and tracking capability for this system as well as other FAA systems including Terminal Doppler Weather Radar (TDWR) and Integrated Terminal Weather System (ITWS). The algorithm utilizes multi-dimensional image processing, data fusion, and fuzzy logic techniques to recognize gust fronts observed in Doppler radar data.

Some deficiencies in algorithm performance have been identified through ongoing analysis of data from two initial limited production WSP sites in Austin, TX (AUS) and Albuquerque, NM (ABQ). At AUS, the most common cause of false alarms is bands of low-reflectivity rain echoes having shapes and intensities similar to gust front thin line echoes. Missed or late detections have occasionally occurred when gust fronts are near or embedded in the leading edge of approaching line storms, where direct radar evidence of the gust front (e.g., thin line echo, velocity convergence) may be fragmented or absent altogether. In ABQ, "canyon wind" events emanating from mountains located just east of the airport occur with very little lead time, and often with little or no radar signatures, making timely detection on the basis of the radar data alone difficult.

MIGFA is equipped with numerous parameters and thresholds that can be adjusted dynamically based on recognition of the local or regional weather context in which it is operating. Through additional contextual weather information processing, this dynamic sensitization capability has been further exploited to address the deficiencies noted above, resulting in an appreciable improvement in performance on data collected at the two WSP sites.

†This work was sponsored by the Federal Aviation Administration under Air Force Contract No. F19628-00-C-0002. The views expressed are those of the authors and do not reflect the official policy or position of the U.S. Government. Opinions, interpretations, conclusions, and recommendations are those of the authors and are not necessarily endorsed by the U.S. Government.

*Corresponding author address: Seth Troxel, MIT Lincoln Laboratory, 244 Wood Street, Lexington, MA 02420-9108; e-mail: setht@ll.mit.edu

2.MIGFA PROCESSING OVERVIEW

Figure 1 is a block diagram illustrating MIGFA processing flow. ASR-9 radar base data products generated by the WSP (reflectivity, Doppler velocity, quality flags) are sent to MIGFA for processing once every 2 minutes. The ASR-9 data extend to a range of 111 km (60 nmi), but gust fronts are reliably detected by the ASR-9 only out to a range of approximately 30 km (15 nmi).

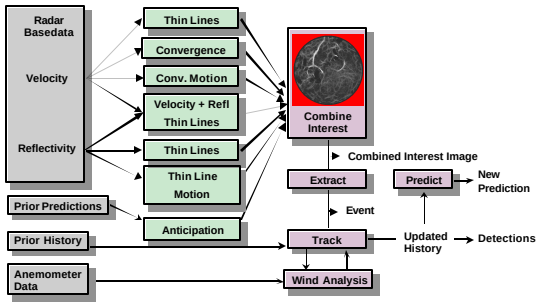

Figure 1. MIGFA Block Diagram

To identify gust fronts, MIGFA runs a series of independent feature detectors that look for radar signatures indicative of gust fronts (e.g., reflectivity thin lines, velocity convergence lines, thin line motion). The feature detectors employ a pattern-matching technique developed at Lincoln Laboratory called Functional Template Correlation (FTC), which through the use of scoring functions (as opposed to flat thresholds) incorporates aspects of fuzzy set theory (Delanoy, 1992). Figure 2 shows an example of FTC used to identify reflectivity thin lines. The output of FTC is a pixel-map of probabilities that the particular feature is present – or not present – in the imagery. The resulting evidence maps, called “interest images”, provide a convenient mechanism for data fusion.

FTC is not the only means by which an interest image may be generated. During the feature detection stage, an “anticipation” interest image is constructed by first filling the interest image with a constant background value that is a function of the amount and type of precipitation present. A higher background anticipation value is chosen when thunderstorms conducive to gust front formation are present. Conversely, a lower background value is chosen when there is considerable low-intensity stratiform precipitation present (a typical

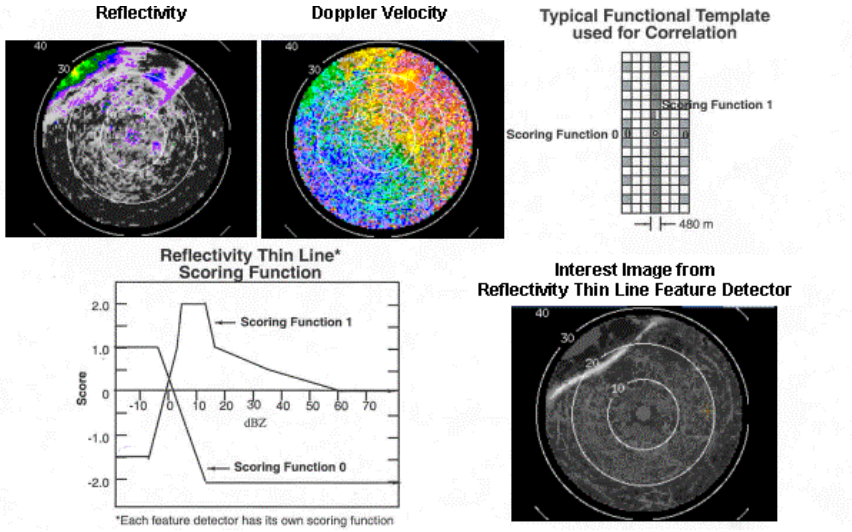

Figure 2. Illustration of Functional Template Correlation (FTC) used to identify a reflectivity thin line signature. The template (upper right) is passed over every pixel of the input reflectivity image (and at several different rotations). The template defines which scoring function (lower left) to use at each relative image location. A score is returned from the selected function based on the underlying image pixel value. The resulting interest image (lower right) indicates locations where a good match was achieved. A corresponding orientation image containing for each pixel the template rotation angle at which the best match occurred is also generated (not shown).

false alarm scenario). Locally high anticipation values are set at image locations where gust fronts are expected based on extrapolations from prior gust front detections. The localized boosting helps support feature detector evidence that might otherwise be too weak to trigger a detection.

Using a confidence-weighted averaging scheme, the individual interest images are fused to form a combined interest image that represents a probabilistic consensus regarding the presence or absence of gust fronts at each pixel location. Gust front chains are extracted by thresholding the combined interest image and performing additional operations to smooth and thin the interest pixels to a single pixel wide chain of points. The candidate gust front chains are then subjected to a series of heuristics to ensure their validity. Point-by-point correspondence is established with gust front chains extracted on prior scans in order to establish a track. The tracking motion estimates are then used to generate predictions of future gust front locations at 1-minute increments out to 30 minutes (for ATC planning purposes, the 10- and 20-minute predictions are shown on the graphical situation display along with the current location of the front). The predictions are also used in the formation of the anticipation image as discussed above.

3. ALGORITHM ENHANCEMENTS

Previous versions of the WSP MIGFA considered data only within the nominal 30 km gust front detection range. However, additional information obtained from processing of the full 111 km range of data has been found to provide very useful contextual cueing information such as improved classification of general precipitation regime, recognition of approaching line storms, and determination of mid-level ambient winds that control general precipitation echo movement.

3.1 Dynamic Sensitivity Adjustment Based on Precipitation Regime

MIGFA's sensitivity is dynamically adjusted (via the anticipation interest image) based on the type and extent of weather within its processing range. If there is a predominance of convective weather (high reflectivity areas), then conditions are favorable for gust fronts and MIGFA's overall sensitivity is heightened by raising the background anticipation level. Conversely, during episodes of widespread low-reflectivity light rain (stratiform rain), gust fronts are not expected. Moreover, the potential for false alarms increases owing to light rain echoes that may occasionally organize in moving bands that mimic gust front thin line echoes. Therefore, it is desirable to reduce MIGFA's sensitivity during these conditions.

Precipitation coverage estimates of convective storm cells and stratiform rain are made by tallying the number of pixels in the full 111 km range reflectivity image that fall within reflectivity bounds assigned to these classes (the bounds are site-adaptable parameters). The tallies are scaled to range from 0 to 10, and are used to index an 11x11 look-up table that returns the background anticipation interest value as a function of convective and stratiform weather coverage.

3.2 Increased Sensitization Near Line Storms

Line storms – organized lines of thunderstorm cells – are favored locations for gust fronts. FTC is used to generate a line storm interest image and corresponding orientation image from the long-range reflectivity image. The interest image is not averaged with the other feature detector interest images, but rather it is used in two ways:

Selected feature detectors consult the pre-computed line storm interest image and associated orientation image. Feature detector interest values that are in the vicinity of line storm regions and which have similar orientations to the line storms (as given by the line storm orientation image) are boosted by a scale factor.

The line storm interest image is used as a mask in the anticipation interest computation to perform additional localized boosting of anticipation for fronts that are currently being tracked in the vicinity of a line storm. This helps reduce the likelihood of losing an established gust front track due to momentary loss of radar signatures.

3.3 Steering Wind Estimation for Rejection of Moving Rain Bands

Gust front false alarms that arise from low reflectivity rain echoes moving with the mid-level ambient winds present a problem for MIGFA that is less tractable than the problem of false alarms arising from spatially stable low reflectivity echoes. This can be a significant problem in environments such as AUS, which are subject to the effects of organized synoptic weather systems. The reason for the lack of tractability is that in the case of moving rain echoes, the reflectivity motion detector will often claim strong evidence for the presence of gust fronts. (This detector looks for thin line signatures in an image that is the pixel-wise difference of the current and previous reflectivity images; thus, this detector looks for evidence of the motion of reflectivity thin line echoes.) Our solution to this problem consists of suppressing evidence of gust fronts when that evidence is moving with the ambient winds (as indicated by the reflectivity motion detector's orientation image – see Figure 2). Specific conditions that are required for such suppression are: confidence in the ambient wind calculation, and little or no evidence of the presence of storm cells.

The ambient wind field is calculated using a modification of the method of least squares called the Gauss-Markov technique (Luenberger, 1969). One begins with a gridded sample of points in the Doppler velocity image associated with the full 111 km range of data, and regresses from this data to a single vector estimate of the ambient wind field. The Gauss-Markov modification to this regression computes, along with the ambient wind estimate, a confidence factor, which provides a sense of the variability of the gridded data, as well as a sense of the signal-to-noise ratio in that data. The extent to which gust front evidence is suppressed varies directly with the confidence value associated with the wind field calculation. This suppression also varies inversely with the level of convective weather coverage, as determined by the method described in Section 3.1. (In the presence of storms, the likelihood of gust fronts becomes high enough as to render this wind field-based suppression counterproductive.)

3.4 Use of Airport Anemometer Network Data

In dry environments like ABQ, radar returns have relatively low signal-to-noise/clutter ratio, and this is reflected in weakness of gust front evidence provided by the MIGFA feature detectors. Even in the presence of such pronounced wind shifts as the Albuquerque "canyon wind" events, which funnel westward through the Sandia Mountains to the east of Albuquerque, MIGFA may fail to make a detection. Our solution in such cases consists of relying on anemometer data, which MIGFA already ingests for use in helping to ensure the validity of gust front candidates that have already been identified by the feature detectors (see Section 2). We now use the anemometer data as an aid in making detections, as well. MIGFA has been enhanced with a detection module, the Low Level Wind (LLWIND) detection module, which, working in parallel with the feature detectors, computes the likely presence of gust fronts using anemometer data.

There are two components of the LLWIND module. The first component detects wind convergence in the anemometer network using techniques similar to the LLWAS (Low Level Windshear Alert System) convergence detection algorithm (Wilson, 1991). When such convergence is detected, thresholds are lowered in the feature detectors to render these detectors more sensitive. The second component of the LLWIND module looks for strong temporal changes in the velocities reported by the individual anemometers. When such a change occurs in the presence of network convergence, MIGFA synthesizes a gust front detection by using the alarming anemometer's location and current value to estimate the position and velocity of the front being synthesized. These strategies often result in the detection of a gust front crossing the anemometer network envelope, which would otherwise go undetected from radar evidence alone.

4. RESULTS

Table 1 compares the performance of MIGFA before and after the enhancements described above, on two test suites of cases. Each case represents real radar and anemometer data, typically one to two hours in length. A variety of weather conditions is represented, which taken as a whole presents a more challenging task for MIGFA than the average weather encountered at either AUS or ABQ.

The data have been truthed by hand. Each truthed gust front is represented in any given scan of data by a polygonal outline called a truth box, and it is considered, when MIGFA makes a gust front prediction, that a correct detection has been made if that prediction lies at least partially within such a truth box. If MIGFA makes

a prediction that lies within no such truth box, that prediction is deemed to be a false alarm.

The significant increase in POD (probability of detection) rate that we see in AUS is attributable to the additional weather context that has been made available to MIGFA through processing of the full 111 km range of radar data, as described in Sections 3.1 and 3.2. The dramatic reduction in probability of false alarms (PFA) is partly attributable to the direct effect of the additional weather context, as well as the indirect effect of this context as embodied in the steering wind-based suppression technique described in Section 3.3.

The equally dramatic POD increase in the ABQ test suite is due primarily to the anemometer-based methods described in Section 3.4. The increase in PFA in ABQ is also attributable to the anemometer-based technique, but this small increase is more than tolerable in light of the POD gain.

Table 1. MIGFA Performance Comparsions for AUS and ABQ Test Suites

AUS (36 cases)	POD	PFA
Baseline MIGFA	58.0	37.1
Enhanced MIGFA	64.2	13.1
ABQ (23 cases)	POD	PFA
Baseline MIGFA	50.1	2.3
Enhanced MIGFA	72.4	5.2

5. SUMMARY AND CONCLUSIONS

MIGFA was first developed to meet the needs for a gust front detection capability for the ASR-9 WSP more than ten years ago (Delanoy, 1993). The multi-dimensional pattern recognition, data fusion, and fuzzy logic techniques that were utilized represented a significant improvement over previous automated gust front detection algorithms. Following the early success with the ASR-9 WSP implementation, versions of MIGFA were soon developed for TDWR and NEXRAD. MIGFA is the gust front algorithm currently operating at all TDWR sites, and will also be the gust front algorithm for the Integrated Terminal Weather System (ITWS) presently being deployed by FAA at major airports in the U.S.

The latest round of improvements has focused on incorporating additional weather context into the algorithm. Providing the WSP MIGFA with a more regional view of the weather through processing of the full 111 km range of the ASR-9 data has proven to be very beneficial in allowing MIGFA to more optimally adjust its dynamic sensitivity. The longer range data have also permitted estimation of precipitation steering winds. This information allows MIGFA to better discriminate thin, light rain echoes from true gust front thin lines, thereby reducing false alarms. Additional processing of data from existing airport anemometer networks provide improved local weather context that aid MIGFA in recognizing gust fronts during conditions where signals are too weak for recognition from the radar data alone.

MIGFA's data fusion framework allows for these kinds of contextual processing enhancements, as well as future improvements, to be easily incorporated into the algorithm. Lincoln Laboratory continues to monitor MIGFA performance at various field sites in the US, and to work on solutions for observed deficiencies.

6. REFERENCES:

Delanoy, R.L., J.G. Verly, and D.E. Dudgeon, 1992: "Functional templates and their application to 3-D object recognition," Proceedings of the 1992 International Conference of Acoustics, Speech, and Signal Processing, San Francisco, CA, pp. 23-26.

Delanoy, R.L., and S.W. Troxel, 1993: "Machine intelligent gust front detection," Massachusetts Institute of Technology, Lincoln Laboratory, *The Lincoln Laboratory Journal*, Vol. 6, No. 1, pp. 187-211.

Luenberger, D. G., 1969: *Optimization by Vector Space Methods,* John Wiley & Sons, Inc.

Troxel, S.W., and R.L. Delanoy, 1994: "Machine intelligent approach to automated gust front detection for Doppler weather radars," SPIE Proceedings: Sensing, Imaging, and Vision for Control and Guidance of Aerospace Vehicles, Volume 2220, pp. 182-193.

Troxel, S.W., R.L. Delanoy, J.P. Morgan, W.L. Pughe, 1996: "Machine intelligent gust front algorithm for the Terminal Doppler Weather Radar (TDWR) and Integrated Terminal Weather System (ITWS)," AMS Workshop on Wind Shear and Wind Shear Alert Systems, Oklahoma City, OK, pp. 70-79.

Wilson, Jr., F.W., R.H. Gramzow, 1991: "The redesigned low level wind shear alert system," Preprints of the Fourth International Conference on Aviation Weather Systems, Paris, France, pp. 370-375.